Ornithine decarboxylase regulates M1 macrophage activation and mucosal inflammation via histone modifications

Dana M. Hardbower[a,b], Mohammad Asim[b], Paula B. Luis[c], Kshipra Singh[b], Daniel P. Barry[b], Chunying Yang[d,e], Meredith A. Steeves[e], John L. Cleveland[d,e], Claus Schneider[c], M. Blanca Piazuelo[b], Alain P. Gobert[b], and Keith T. Wilson[a,b,f,g,h,1]

[a]Department of Pathology, Microbiology and Immunology, Vanderbilt University Medical Center, Nashville, TN 37232; [b]Division of Gastroenterology, Hepatology and Nutrition, Department of Medicine, Vanderbilt University Medical Center, Nashville, TN 37232; [c]Department of Pharmacology, Vanderbilt University School of Medicine, Nashville, TN 37232; [d]Department of Tumor Biology, Moffitt Cancer Center and Research Institute, Tampa, FL 33612; [e]Department of Cancer Biology, The Scripps Research Institute, Jupiter, FL 33458; [f]Department of Cancer Biology, Vanderbilt University School of Medicine, Nashville, TN 37232; [g]Center for Mucosal Inflammation and Cancer, Vanderbilt University Medical Center, Nashville, TN 37232; and [h]Veterans Affairs Tennessee Valley Healthcare System, Nashville, TN 37232

Edited by Carl F. Nathan, Weill Medical College of Cornell University, New York, NY, and approved December 20, 2016 (received for review September 6, 2016)

Macrophage activation is a critical step in host responses during bacterial infections. Ornithine decarboxylase (ODC), the rate-limiting enzyme in polyamine metabolism, has been well studied in epithelial cells and is known to have essential roles in many different cellular functions. However, its role in regulating macrophage function during bacterial infections is not well characterized. We demonstrate that macrophage-derived ODC is a critical regulator of M1 macrophage activation during both *Helicobacter pylori* and *Citrobacter rodentium* infection. Myeloid-specific *Odc* deletion significantly increased gastric and colonic inflammation, respectively, and enhanced M1 activation. Add-back of putrescine, the product of ODC, reversed the increased macrophage activation, indicating that ODC and putrescine are regulators of macrophage function. *Odc*-deficient macrophages had increased histone 3, lysine 4 (H3K4) monomethylation, and H3K9 acetylation, accompanied by decreased H3K9 di/trimethylation both in vivo and ex vivo in primary macrophages. These alterations in chromatin structure directly resulted in up-regulated gene transcription, especially M1 gene expression. Thus, ODC in macrophages tempers antimicrobial, M1 macrophage responses during bacterial infections through histone modifications and altered euchromatin formation, leading to the persistence and pathogenesis of these organisms.

macrophage polarization | polyamines | histone modifications | ornithine decarboxylase | *Helicobacter pylori*

Polyamine metabolism is a process critical for life occurring within all mammalian cell types (1, 2). Polyamines have ubiquitous roles in many cellular functions, including growth, proliferation, and differentiation (1). Importantly, polyamines have also been implicated in the alteration of histone modifications and chromatin structure and thus might broadly affect DNA stability and transcription (3–5). The production of the three major polyamines—putrescine, spermidine, and spermine—is tightly regulated and centers on the rate-limiting enzyme, ornithine decarboxylase (ODC1, hereafter referred to as ODC) (2, 6). ODC uses the substrate, L-ornithine, to produce putrescine via a decarboxylation reaction (2, 6). Given its essential and central role in regulating polyamine metabolism within cells, ODC has been highly studied and implicated in several malignancies, including breast, colorectal, and gastric cancer (7–11). However, most of the studies related to ODC have been focused on its role in epithelial cell function, leaving many questions surrounding the role of ODC in immune cells unanswered.

In particular, macrophages are a significant component of the innate immune cell compartment and play wide-ranging roles in immune surveillance, responses to pathogens, wound healing, embryonic development, and regulation of the tumor microenvironment (12, 13). An essential step in the responses to pathogens is macrophage activation. Macrophages have the capacity to alter cytokine/chemokine production and various other functions along the spectrum of M1 or M2 activation based on the stimulus detected (12–14). M1 macrophages represent a highly proinflammatory and antimicrobial subset of macrophages (12–14). M2 macrophages have various roles in wound repair, antiparasitic responses, control of inflammation, and have been implicated in tumor development and growth (15–18). The role of ODC has been well characterized in M2 macrophage responses to various parasitic and fungal infections (19–21), but the role of ODC in macrophages during M1 responses has been less well studied (22). We have demonstrated that ODC expression is up-regulated during bacterial infections (23–26), but the role in macrophage activation patterns requires further investigation.

To address this question, we used *Helicobacter pylori*, a globally pervasive human pathogen that represents the single greatest risk factor in the development of gastric cancer (27–30). *H. pylori* establishes a chronic infection in humans, which can be recapitulated in mice (14), marked by continuous, low-grade inflammation and host tolerance of the pathogen (31–34). We also used the *Citrobacter rodentium* infectious colitis model (26, 35). *C. rodentium*

Significance

The pathogenesis of many bacteria is enhanced by the ability to establish persistent infection. Macrophages, particularly classically activated M1 macrophages, provide essential functions in the initiation of antibacterial immune responses. The regulation of macrophage activation is still poorly understood. Here, we demonstrate that ornithine decarboxylase (ODC), the rate-limiting enzyme in polyamine synthesis, regulates M1 activation during *Helicobacter pylori* and *Citrobacter rodentium* infection. Deletion of *Odc* in macrophages resulted in increased inflammation and decreased bacterial persistence in mouse models. The enhanced M1 response was due to alterations in histone modifications, resulting in changes in chromatin structure and up-regulated transcription. These findings represent a novel mechanism by which ODC directly regulates macrophage activation and provides new insights into understanding bacterial persistence.

Author contributions: D.M.H., A.P.G., and K.T.W. designed research; D.M.H., M.A., P.B.L., K.S., C.S., and M.B.P. performed research; D.P.B., C.Y., M.A.S., and J.L.C. contributed new reagents/analytic tools; D.M.H. and K.T.W. analyzed data; and D.M.H. and K.T.W. wrote the paper.

The authors declare no conflict of interest.

This article is a PNAS Direct Submission.

[1]To whom correspondence should be addressed. Email: keith.wilson@vanderbilt.edu.

This article contains supporting information online at www.pnas.org/lookup/suppl/doi:10.1073/pnas.1614958114/-/DCSupplemental.

is an enteric bacterial pathogen that forms attaching and effacing lesions in the colon and is similar to enteropathogenic *Escherichia coli* infection in humans (36). As macrophages are known to have a critical role in *H. pylori*-mediated gastritis (14, 37) and *C. rodentium* colitis (14), we sought to interrogate the specific role of ODC in macrophages during these enteric infections, using a myeloid/macrophage-specific *Odc* knockout mouse.

In this study, we have uncovered a mechanism by which ODC and its product, putrescine, regulates macrophage activation and function. We show that macrophage-derived ODC plays a critical role in the inhibition of M1 macrophage activation to promote persistence of infection. This defect in M1 macrophage activation is directly regulated by polyamine production that modulates chromatin structure, as determined by alterations in histone modification markers in vitro and in vivo, which prevents proinflammatory gene transcription.

Results

Myeloid-Specific ODC Deletion Enhances Gastritis and Bacterial Killing During *H. pylori* Infection. As we have previously demonstrated that ODC plays a significant role in macrophage function during *H. pylori* infection in vitro (24, 25, 38), we hypothesized that macrophage-derived ODC would have significant effects on *H. pylori* pathogenesis, specifically in the regulation of gastric inflammation. As *H. pylori* is a human pathogen, we first assessed ODC levels in mononuclear cells in gastric biopsies from patients from Colombia infected with *H. pylori* with chronic active gastritis, where overall risk of gastric cancer is high (39, 40). We found that *H. pylori* infection leads to a significant increase in ODC levels in mononuclear cells, which includes abundant expression in cells with the appearance of macrophages (Fig. 1 *A* and *B*).

To confirm that human macrophages express increased ODC during *H. pylori* infection, we performed immunofluorescence staining for ODC and CD68, a macrophage marker, on a subset of the cases from Colombia. Control staining in which no primary anti-ODC antibody was used was performed to confirm the specificity of the staining (*SI Appendix*, Fig. S1*A*). As expected, the number of $CD68^+$ macrophages was increased in the *H. pylori*$^+$ cases compared with the normal cases (*SI Appendix*, Fig. S1*B*). Whereas there was no difference in the number of $CD68^+ODC^-$ macrophages between normal and *H. pylori*$^+$ cases (*SI Appendix*, Fig. S1*C*), we found a significant increase in the number of $CD68^+ODC^+$ cells in the *H. pylori*-infected cases versus control

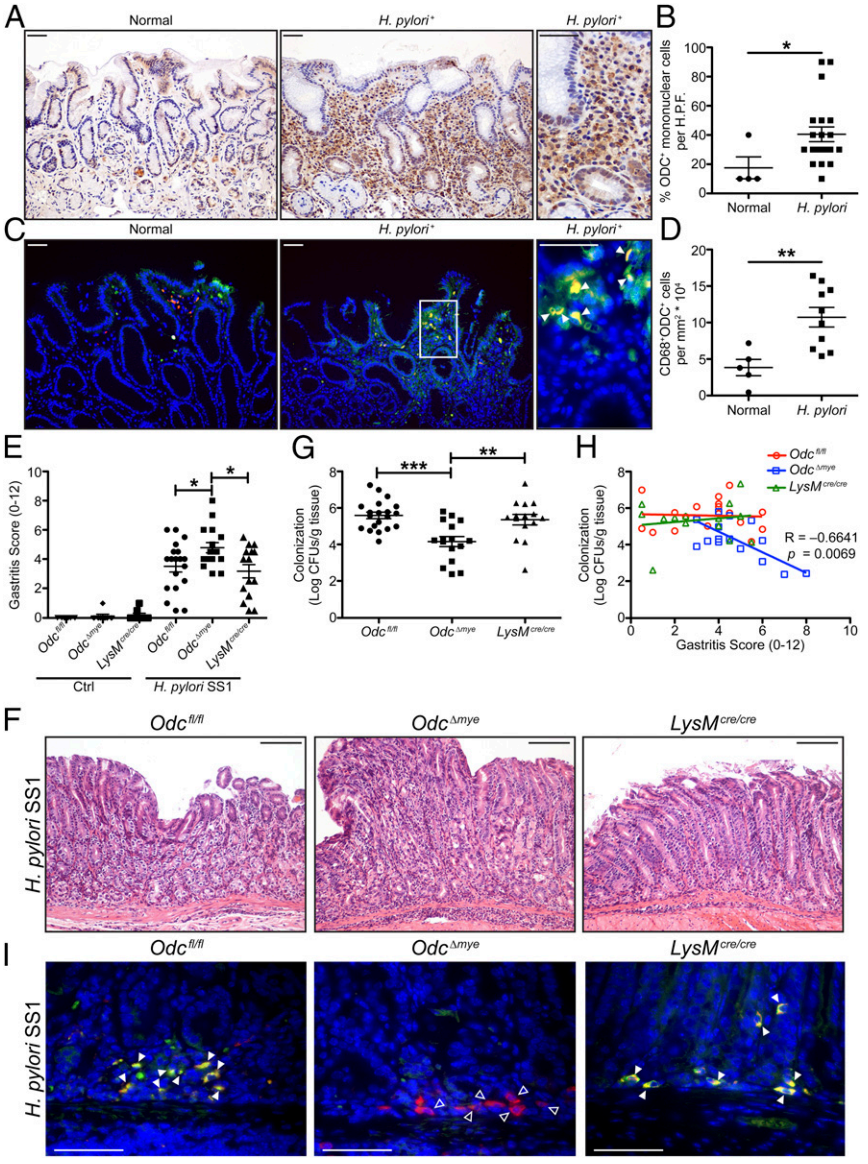

Fig. 1. *Odc*$^{\Delta mye}$ mice have significantly increased histologic gastritis, but significantly decreased *H. pylori* burden after chronic infection. (*A*) Representative immunoperoxidase staining for ODC in human gastric biopsies from patients with normal mucosa and with *H. pylori*$^+$ gastritis. (Scale bars, 50 μm.) (*B*) Quantification of the percentage of ODC^+ mononuclear cells in gastric biopsies from *A*. $n = 4$ normal biopsies and 20 *H. pylori*$^+$ gastric biopsies with chronic active gastritis. $^*P < 0.05$ by Mann–Whitney *u* test. H.P.F., high power field. (*C*) Representative immunofluorescence images of ODC from gastric biopsies in *A* and *B*. Green, ODC; red, CD68; yellow, merge; and blue, DAPI. Closed arrows indicate $CD68^+ODC^+$ macrophages. Boxed area indicates image shown in higher magnification. (Scale bars, 50 μm.) Note that different cases were used for representative images in *A* and *C*. (*D*) Quantification of the number of $CD68^+ODC^+$ cells in the cases from *C*. $n = 5$ normal biopsies and 10 *H. pylori*$^+$ gastric biopsies with chronic active gastritis. $^{**}P < 0.05$ by Student's *t* test. (*E*) Histologic gastritis scores were assessed 4 mo p.i. by a gastrointestinal pathologist in a blinded manner according to the updated Sydney System. (*F*) Representative H&E images from infected mice in *E*. (Scale bars, 100 μm.) (*G*) Colonization of *H. pylori* SS1 was assessed by serial dilution and culture 4 mo p.i. In *E* and *G*, $^*P < 0.05$, $^{**}P < 0.01$, $^{***}P < 0.001$ by one-way ANOVA with Newman–Keuls posttest. $n = 8$–10 uninfected and 15–19 *H. pylori* SS1-infected mice per genotype. (*H*) Correlation between histologic gastritis in *E* and *H. pylori* SS1 colonization levels in *G*. Correlation and significance determined by Pearson's product-moment correlation test. (*I*) Representative immunofluorescence images of ODC from infected mice in *E* and *G*. Green, ODC; red, CD68; yellow, merge; and blue, DAPI. Closed arrows indicate $CD68^+ODC^+$ macrophages. Open arrows indicate $CD68^+ODC^-$ macrophages. (Scale bars, 50 μm.) Data are displayed as mean ± SEM.

cases (Fig. 1 *C* and *D*). Moreover, the percentage of $CD68^+ODC^+$ macrophages per total number of $CD68^+$ macrophages was significantly higher in *H. pylori*$^+$ cases (*SI Appendix*, Fig. S1*D*). These data indicate that *H. pylori* infection is associated with up-regulated ODC in human gastric macrophages, which led us to hypothesize that ODC has an important role in regulating macrophage function during infection.

To further investigate the role of macrophage-derived ODC, we generated mice with a myeloid-specific deletion of *Odc*, by crossing C57BL/6 $Odc^{fl/fl}$ mice with myeloid-specific $LysM^{cre/cre}$ driver mice, yielding the $Odc^{\Delta mye}$ mouse (*SI Appendix*, Fig. S2*A*). We assessed *Odc* mRNA levels in $CD11b^+$ myeloid cells and $CD11b^-$ non-myeloid cells from the gastric lamina propria of mice infected with *H. pylori* premouse Sydney strain 1 (PMSS1) for 48 h, the peak of gastric macrophage infiltration (6, 41), as well as in gastric epithelial cells (GECs). Importantly, only the $CD11b^+$ lamina propria cells demonstrated induction of *Odc* during *H. pylori* infection, which was ablated in $Odc^{\Delta mye}$ $CD11b^+$ cells (*SI Appendix*, Fig. S2*B*). Notably, *Odc* was not induced in $CD11b^-$ cells or GECs, and *Odc* mRNA levels were not altered in these cells derived from the $Odc^{fl/fl}$ and $Odc^{\Delta mye}$ mice (*SI Appendix*, Fig. S1*C*), consistent with the specificity of the knockout. We also demonstrated sufficient *Odc* knockdown in primary bone-marrow–derived macrophages (BMmacs) by real-time (RT)-PCR and Western blotting during *H. pylori* infection (*SI Appendix*, Fig. S2 *C*–*E*).

Additionally, expression levels of lysozyme 2 (*Lyz2*, *LysM*), the gene on which the causes recombination (CRE) recombinase was placed, and *Cre* were assessed in *H. pylori* Sydney strain 1 (SS1)-infected gastric tissues and in *H. pylori* PMSS1-infected BMmacs from $Odc^{fl/fl}$, $Odc^{\Delta mye}$, and $LysM^{cre/cre}$ mice. At 4 mo postinfection (p.i.), gastric *Lyz2* mRNA was nearly undetectable, whereas *Cre* mRNA was abundant in both infected and uninfected $Odc^{\Delta mye}$ gastric tissue (*SI Appendix*, Fig. S3*A*). Conversely, *Lyz2* was induced upon infection in $Odc^{fl/fl}$ gastric tissues and no *Cre* was detected (*SI Appendix*, Fig. S3*A*). These data were recapitulated in BMmacs from $Odc^{fl/fl}$, $Odc^{\Delta mye}$, and $LysM^{cre/cre}$ mice (*SI Appendix*, Fig. S3*B*). The maintenance of the *Lyz2* deletion and of high *Cre* expression during acute and chronic infection confirms the durability of the *Odc* deletion over time (14).

Upon confirmation of *Odc* knockdown in myeloid cells, $Odc^{fl/fl}$, $Odc^{\Delta mye}$, and $LysM^{cre/cre}$ mice were investigated for their response to infection with *H. pylori* SS1 for 4 mo, a model of chronic *H. pylori* infection (14, 25, 42). $Odc^{\Delta mye}$ mice demonstrated significantly enhanced acute and chronic histologic gastritis, compared with either $Odc^{fl/fl}$ or $LysM^{cre/cre}$ mice (Fig. 1 *E* and *G*). Consistent with previous studies (14, 23, 34, 43) in which colonization and gastritis are typically inversely related, the enhanced gastritis was correlated with significantly decreased *H. pylori* burden in $Odc^{\Delta mye}$ mice (Fig. 1 *G* and *H*), indicating that ODC has an important role in regulating antimicrobial inflammation in the stomach. Importantly, there were no detectable phenotypic differences between the $Odc^{fl/fl}$ or $LysM^{cre/cre}$ mice, confirming all phenotypes are being driven by *Odc* deletion (Fig. 1 *E*–*H*).

ODC knockout was confirmed by immunofluorescence in $CD68^+$ gastric macrophages from chronically infected gastric tissues from $Odc^{fl/fl}$, $Odc^{\Delta mye}$, and $LysM^{cre/cre}$ mice. ODC colocalized with $CD68^+$ macrophages in both $Odc^{fl/fl}$ and $LysM^{cre/cre}$ gastric tissues, whereas ODC was not expressed in $CD68^+$ cells in $Odc^{\Delta mye}$ gastric tissues (Fig. 1*H*). Control staining in which no primary anti-ODC antibody was used confirmed the specificity of the immunofluorescence (*SI Appendix*, Fig. S4). These data further confirmed successful deletion of *Odc* in macrophages, as well as maintenance of the knockout over time and during infection.

We next sought to determine whether the role of ODC in macrophages was specific to *H. pylori* pathogenesis. *Odc* expression was also up-regulated in BMmacs exposed to *C. rodentium* and was markedly attenuated in $Odc^{\Delta mye}$ BMmacs (*SI Appendix*, Fig. S5*A*). $Odc^{fl/fl}$ and $Odc^{\Delta mye}$ mice were inoculated with *C. rodentium* for 14 d. As in the chronic *H. pylori* model, $Odc^{\Delta mye}$ mice exhibited significantly increased levels of histologic inflammation and injury, represented by higher colitis scores, compared with $Odc^{fl/fl}$ mice (*SI Appendix*, Fig. S5 *B* and *C*). Moreover, tissues from $Odc^{\Delta mye}$ mice had increased colon weight as a percentage of body weight on the day of killing (*SI Appendix*, Fig. S5*D*), which is a marker of increased disease severity (35). The significant increases in colitis and disease severity were concordant with the increased histologic gastritis observed in the *H. pylori* model, indicating that the role of ODC in regulating macrophage activation responses is conserved across various bacterial infections. However, differences in *C. rodentium* burden were not detected in colonic tissues between $Odc^{fl/fl}$ and $Odc^{\Delta mye}$ mice (*SI Appendix*, Fig. S5*E*); this finding is consistent with our prior reports that, whereas diminished immune response can result in increased colonization (14, 44), increased inflammation does not lead to decreased colonization in this model (45).

ODC Deletion Augments Proinflammatory Cytokine and Chemokine Production in Vivo. Our in vivo findings demonstrated that macrophage-derived ODC has an antiinflammatory role during bacterial pathogenesis. Thus, we hypothesized that the loss of ODC in macrophages leads to enhanced innate immune responses to *H. pylori*. We used a Luminex multiplex array to assess 25 distinct chemokines and cytokines in gastric tissues from chronically infected $Odc^{fl/fl}$, $Odc^{\Delta mye}$, and $LysM^{cre/cre}$ mice. Nine analytes were significantly increased at the protein level in *H. pylori*-infected $Odc^{\Delta mye}$ gastric tissues, compared with $Odc^{fl/fl}$ or $LysM^{cre/cre}$ gastric tissues. C-C motif ligand (CCL) chemokines, CCL2 (MCP-1), CCL3 (MIP-1α), CCL4 (MIP-1β), and CCL5 (RANTES), and C-X-C motif ligand (CXCL) chemokines, CXCL1 (GROα, KC), CXCL2 (MIP2), and CXCL10 (IP-10), were all significantly increased in $Odc^{\Delta mye}$ gastric tissues (Fig. 2). The enhanced chemokine production suggests that the deletion of macrophage ODC has a role in enhancing immune cell infiltration into the stomach, contributing to the significantly increased inflammation. Additionally, the cytokines interleukin (IL)-17 and tumor necrosis factor (TNF)-α were detected at significantly higher levels in $Odc^{\Delta mye}$ gastric tissues at 4 mo p.i. (Fig. 2). IL-17 is a hallmark of the Th17 response (46), especially in *H. pylori* infection (14), indicating an enhanced proinflammatory T-cell response to *H. pylori* and a diminished ability to control infection (47) under conditions of macrophage *Odc* deletion. Many cell types can produce TNF-α, especially M1-activated macrophages (12). Analytes that were not induced by infection in any of the genotypes, were not significantly different between genotypes, or were not detected are listed in *SI Appendix*, Table S1.

ODC Deletion Leads to Enhanced M1 Macrophage Activation During Bacterial Infections. The increased TNF-α levels in the context of myeloid-specific *Odc* deletion led us to hypothesize that ODC normally serves to suppress M1 macrophage activation. Thus, enhanced M1 responses in $Odc^{\Delta mye}$ mice would have the potential to orchestrate the highly proinflammatory immune response to both *H. pylori* and *C. rodentium*. To test our hypothesis, we expanded upon a previously used panel of genes marking M1 and M2 macrophage activation (14, 23) and assessed expression levels of each marker in chronically infected gastric tissues from $Odc^{fl/fl}$, $Odc^{\Delta mye}$, and $LysM^{cre/cre}$ mice. mRNA expression of M1 activation markers, *Il1b*, *Il6*, *Il12a* (*Il12p35*), *Il12b* (*Il12p40*), *Tnfa*, and nitric oxide synthase 2 (*Nos2*), were induced during *H. pylori* infection in gastric tissues from each genotype (Fig. 3*A*). Expression of each of these genes was markedly increased in $Odc^{\Delta mye}$ versus $Odc^{fl/fl}$ or $LysM^{cre/cre}$ gastric tissues (Fig. 3*A*). Additionally, *C. rodentium*-infected colonic tissues demonstrated an induction of M1 marker expression that was further increased in $Odc^{\Delta mye}$ colonic tissues (*SI Appendix*, Fig. S6*A*). Taken together, these data demonstrate that the loss of ODC in myeloid cells significantly magnifies M1 macrophage activation in response to bacterial enteric pathogens.

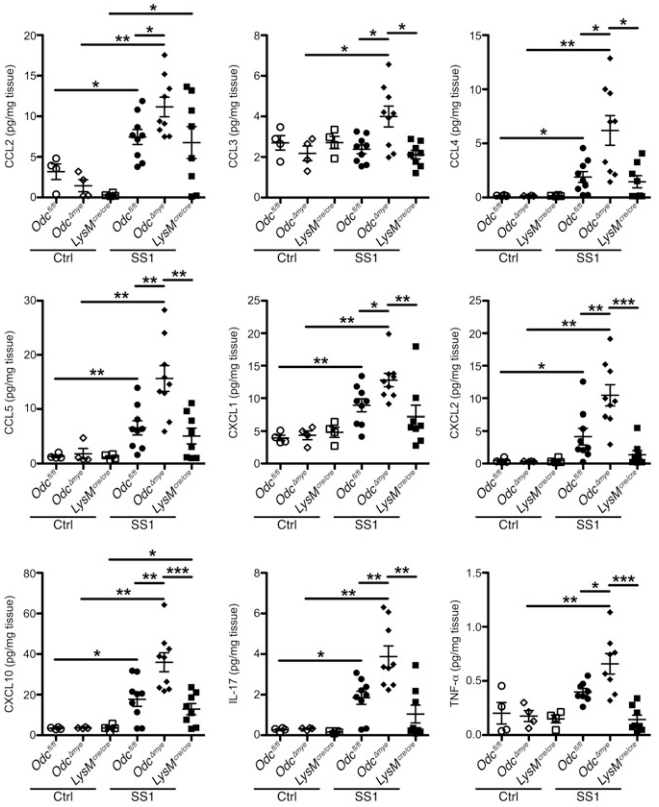

Fig. 2. Cytokines and chemokines are significantly increased in $Odc^{\Delta mye}$ gastric tissues. Protein levels of the cytokines and chemokines CCL2 (MCP-1), CCL3 (MIP-1α), CCL4 (MIP-1β), CCL5 (RANTES), CXCL1 (KC/GRO-α), CXCL2 (MIP-2), CXCL10 (IP-10), IL-17, and TNF-α were assessed by Luminex multiplex array in gastric tissues 4 mo p.i. with *H. pylori* SS1. $*P < 0.05$, $**P < 0.01$, $***P < 0.001$ by one-way ANOVA with Kruskal–Wallis test, followed by Mann–Whitey *u* test. $n = 4$ uninfected and 8–9 *H. pylori* SS1-infected mice per genotype. Data are displayed as mean ± SEM.

Markers of M2 activation were also assessed in gastric and colonic tissues from *H. pylori*-infected mice. The following panel of M2 markers was used: arginase 1 (*Arg1*), chitinase-like 3 (*Chil3*, *Ym1*), resistin-like a (*Retnla*, *Relma*), *Il10*, transforming growth factor-b (*Tgfb*) 1, and tumor necrosis factor (ligand) superfamily member 14 *(Tnfsf14*; *Light*). *H. pylori* infection does not typically induce a robust M2 macrophage response (14, 23). Indeed, M2 genes *Arg1*, *Chil3*, *Retnla*, *Il10*, and *Tgfb1* were not significantly induced in $Odc^{fl/fl}$ or $LysM^{cre/cre}$ gastric tissues (*SI Appendix*, Fig. S7*A*). *Tnfsf14* was significantly induced in $Odc^{fl/fl}$ and $LysM^{cre/cre}$ gastric tissues, but was significantly decreased in $Odc^{\Delta mye}$ gastric tissues (*SI Appendix*, Fig. S7*A*). Because *Tnfsf14* was the only M2 gene up-regulated in infected gastric tissues, these data indicate that *H. pylori* infection does not induce a significant M2 response in mice during chronic infection.

Interestingly, $Odc^{\Delta mye}$ mice demonstrated enhanced *Arg1* expression in whole gastric tissue during *H. pylori* infection (*SI Appendix*, Fig. S7*A*); ARG1 is upstream of ODC and its up-regulation may potentially represent a response to the loss of putrescine production by ODC in the myeloid-specific *Odc* knockout mice. However, based on previous studies, macrophages are not the likely source of *Arg1* in these tissues (26, 48). Moreover, *Arg1* mRNA levels were significantly higher in $Odc^{\Delta mye}$ GECs than in $Odc^{fl/fl}$ GECs following *H. pylori* infection (*SI Appendix*, Fig. S7*B*), indicating that epithelial cells may be the source of increased *Arg1*. Taken together, these data indicate that ODC does not have a major role in regulating M2 activation, but that *Odc* deletion in macrophages allows for enhanced M1 activation.

To confirm the specificity of these findings to macrophages, we assessed macrophage activation in BMmacs from each of the genotypes infected ex vivo with either *H. pylori* or *C. rodentium*. As in the gastric tissues, *Il1b*, *Il6*, *Il12a*, *Il12b*, *Tnfa*, and *Nos2*, mRNA levels were significantly increased in $Odc^{\Delta mye}$ BMmacs infected with *H. pylori* (Fig. 3*B*). Representative M1 genes, *Il1b*, *Tnfa*, and *Nos2*, were also increased in *C. rodentium*-infected $Odc^{\Delta mye}$ BMmacs (*SI Appendix*, Fig. S8) versus $Odc^{fl/fl}$ or $LysM^{cre/cre}$ BMmacs. Moreover, $Odc^{\Delta mye}$ BMmacs had significantly increased secreted levels of IL-1β, IL-6, IL-12p70, and TNF-α (Fig. 3*C*), as well as increased NOS2 protein levels (Fig. 3*D*) and NO production (Fig. 3*E*) in response to *H. pylori* infection. Densitometry further confirmed the significant increase in NOS2 protein levels in $Odc^{\Delta mye}$ BMmacs (*SI Appendix*, Fig. S9). These data clearly demonstrate enhanced M1 macrophage activation at the functional level in *Odc*-deficient macrophages.

M2 marker gene expression revealed a more complicated picture in *H. pylori*-infected BMmacs. *Arg1*, *Chil3*, *Retnla*, and *Tnfsf14* were not induced by *H. pylori* infection, regardless of genotype (*SI Appendix*, Fig. S10*A*). However, *H. pylori* infection induced *Il10* and *Tgfb1* mRNA expression, which was significantly increased in $Odc^{\Delta mye}$ BMmacs versus the control genotypes (*SI Appendix*, Fig. S10*A*). Protein levels of IL-10 confirmed the mRNA data, whereas TGF-β1 secretion was not altered between genotypes (*SI Appendix*, Fig. S10*B*). As M1 activation was consistently increased in both gastric tissues and BMmacs from $Odc^{\Delta mye}$ mice, and M2 activation was not, these data indicate that ODC is a key regulator of M1 macrophage activation during bacterial infections. In contrast, the potential role of ODC in M2 activation during bacterial infections is much less apparent.

To determine whether the role of ODC was conserved in human macrophages, we used THP1 cells, a human monocytic cell line that can be differentiated into macrophages with phorbol myristate acetate (PMA). We determined that *H. pylori* infection induced ODC expression at the mRNA and protein levels (*SI Appendix*, Fig. S11 *A* and *B*). We then treated THP1 cells with difluoromethylornithine (DFMO), an irreversible and specific ODC inhibitor (25), for 3 or 5 d and then infected them with *H. pylori* PMSS1 for 6 h. We assessed M1 and M2 activation by RT-PCR. DFMO-treated, *H. pylori*-infected THP1 cells had a significant increase in induction of *IL1B*, *IL12A*, *IL12B*, and *TNFA* compared with untreated, *H. pylori*-infected cells (*SI Appendix*, Fig. S11*C*). *IL10* expression was induced by infection, but DFMO treatment did not further alter expression (*SI Appendix*, Fig. S11*D*). Importantly, the data related to M1 marker expression demonstrate that ODC also has a role in regulating M1 activation in human macrophages.

Macrophage activation can occur in many settings beyond the context of bacterial infection (12, 13, 16, 17). We next sought to determine the global role of ODC in macrophage activation in BMmacs by using prototypical stimuli of M1 and M2 activation that are not dependent upon bacterial infection. An M1 response was induced by stimulation with IFN (IFN)-γ and lipopolysaccharide (LPS) (12) and an M2 response was elicited via stimulation with IL-4 (12). M(IFN-γ/LPS) macrophages from $Odc^{\Delta mye}$ mice, as with *H. pylori*- or *C. rodentium*-infected macrophages, demonstrated significantly increased *Il1b*, *Tnfa*, and *Nos2* expression compared with $Odc^{fl/fl}$ or $LysM^{cre/cre}$ BMmacs (*SI Appendix*, Fig. S12*A*). Interestingly, M(IL-4) macrophages from $Odc^{\Delta mye}$ mice had further up-regulation of *Arg1* and *Chil3* (*SI Appendix*, Fig. S12*B*). Thus, ODC has the capacity to regulate subsets of macrophage activation in a stimulus-dependent manner. These data demonstrate the central role of ODC in regulating macrophage activation in general.

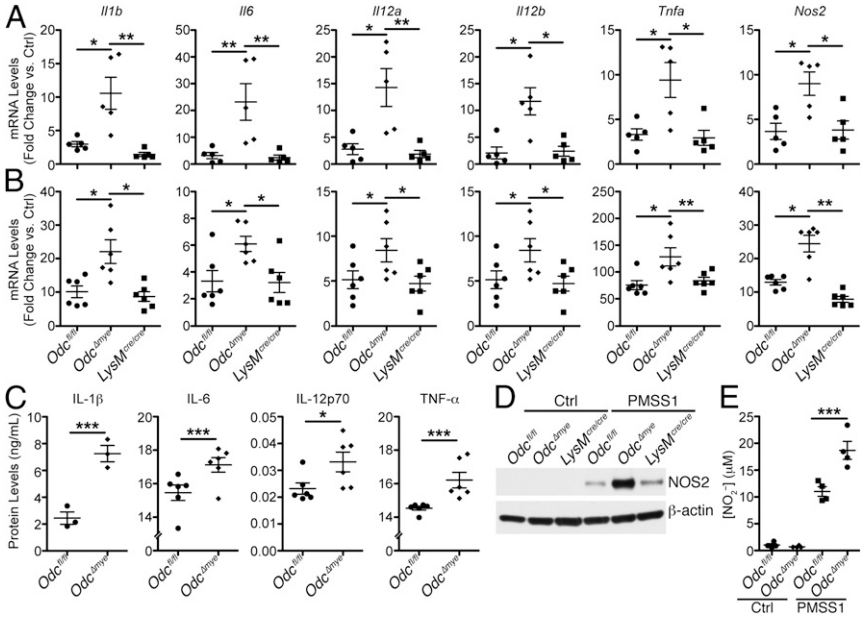

Fig. 3. *Odc* deletion in macrophages enhances M1 macrophage activation during *H. pylori* infection. (*A*) mRNA levels of proinflammatory cytokines *Il1b*, *Il6*, *Il12a*, *Il12b*, *Tnfa*, and the gene *Nos2* were assessed by RT-PCR in gastric tissues 4 mo p.i. with *H. pylori* SS1. $*P < 0.05$, $**P < 0.01$. $n = 3$ uninfected and 5 *H. pylori* SS1-infected mice per genotype. (*B*) mRNA levels of proinflammatory cytokines *Il1b*, *Il6*, *Il12a*, *Il12b*, *Tnfa*, and *Nos2* were assessed by RT-PCR in bone-marrow–derived macrophages (BMmacs) 24 h p.i. with *H. pylori* PMSS1. $*P < 0.05$, $**P < 0.01$. Statistical significance in *A* and *B* was calculated by one-way ANOVA with Kruskal–Wallis test, followed by Mann–Whitney *u* test. $n = 6$ mice per genotype. Note that the *y* axis values for *Il1b*, *Il6*, and *Nos2* have been divided by a factor of 1,000. All samples were analyzed as fold change against $Odc^{fl/fl}$ uninfected control samples. No differences were observed in the fold changes for uninfected samples from all genotypes. (*C*) Secreted levels of IL-1β, IL-6, IL-12p70, and TNF-α were measured by ELISA from supernatants of BMmacs 24 h p.i. with *H. pylori* PMSS1. $*P < 0.05$, $**P < 0.01$ by one-way ANOVA with Newman–Keuls posttest. $n = 3$–6 mice per genotype. Note that none of the cytokines displayed were detected in supernatants from uninfected BMmacs. (*D*) Representative Western blot of NOS2 levels in BMmacs 24 h p.i. with *H. pylori* PMSS1. $n = 3$ biological replicates. (*E*) Measurement of NO_2^- from BMmac supernatants 24 h p.i. with *H. pylori* PMSS1. $***P < 0.001$ by one-way ANOVA with Newman–Keuls posttest. $n = 4$ mice per genotype. Data are displayed as mean ± SEM.

The Role of ODC in Macrophages Is Dependent upon the Polyamine, Putrescine. As the rate-limiting enzyme in polyamine synthesis, ODC converts L-ornithine to the polyamine, putrescine (2, 25, 38), which can then be converted into spermidine and spermine. We determined putrescine, spermidine, and spermine levels by liquid chromatography-mass spectrometry (LC-MS) using deuterated d_8-polyamines as internal standards. Deletion of *Odc* resulted in significantly diminished putrescine and spermidine levels in macrophages at 6 h and 24 h p.i. (Fig. 4*A*). *Odc* deletion resulted in modest spermine accumulation (Fig. 4*A*), which has been demonstrated previously during ODC inhibition with DFMO (11). Moreover, *H. pylori* infection resulted in increased putrescine levels and decreased spermine levels in $Odc^{fl/fl}$ BMmacs at 24 h p.i. (Fig. 4*A*), indicating that infection can modulate polyamine metabolism.

We hypothesized that addition of excess putrescine to the $Odc^{\Delta mye}$ BMmacs would serve to complement the deletion of *Odc* and reverse the enhanced M1 activation during *H. pylori* infection. Indeed, *H. pylori*-stimulated expression of *Nos2*, *Il1b*, and *Tnfa* in $Odc^{\Delta mye}$ BMmacs was no longer statistically increased compared with $Odc^{fl/fl}$ BMmacs when putrescine was added to the cells (Fig. 4*B*). Moreover, the addition of putrescine significantly reduced NO production from infected $Odc^{\Delta mye}$ BMmacs, such that it was no longer significantly higher than NO production from $Odc^{fl/fl}$ BMmacs (Fig. 4*C*). Putrescine had no effect on gene expression in $Odc^{fl/fl}$ BMmacs (Fig. 4 *B*–*D*). Intriguingly, the addition of putrescine had no effect on M2 macrophage activation (*SI Appendix*, Fig. S13), beyond its effect on *Tgfb1* (Fig. 4*D*).

ODC Deletion in Macrophages Also Enhances NLRP3-Inflammasome Activation. IL-1β is the secreted effector protein of the NLR family, pyrin domain containing (NLRP) 3-driven inflammasome (49). As we observed enhanced *Il1b* gene expression, we hypothesized that ODC may also affect NLRP3-inflammasome activation. We first assessed mRNA levels of NLRP3-inflammasome markers—*Nlrp3* and caspase 1 (*Casp1*)—in both gastric tissues and BMmacs from $Odc^{fl/fl}$, $Odc^{\Delta mye}$, and $LysM^{cre/cre}$ mice. As expected, *Nlrp3* and *Casp1* expression was significantly higher in $Odc^{\Delta mye}$ mice during *H. pylori* infection than in the control genotypes in both chronically infected gastric tissue and acutely infected BMmacs (*SI Appendix*, Fig. S14 *A* and *C*). Additionally, the levels of total IL-1β in *H. pylori*-infected gastric tissues were significantly increased in $Odc^{\Delta mye}$ mice (*SI Appendix*, Fig. S14*B*). Both pro–IL-1β (*SI Appendix*, Fig. S14*D*) and secreted IL-1β (Fig. 3*C*) levels were substantially higher in $Odc^{\Delta mye}$ BMmacs. The role of ODC in regulating NLRP3-inflammasome activation is also dependent upon putrescine production, as the addition of excess putrescine substantially decreased *Nlrp3* and *Casp1* expression in $Odc^{\Delta mye}$ BMmacs, such that expression was no longer statistically different from *Nlrp3* and *Casp1* levels in $Odc^{fl/fl}$ BMmacs (*SI Appendix*, Fig. S14*E*). These data indicate that the combination of increased expression of *Il1b* and NLRP3 inflammasome constituents are contributing to increased IL-1β levels. Moreover, IL-1β is a potent proinflammatory cytokine (49) and thus may be substantially contributing to the enhanced histologic gastritis observed in $Odc^{\Delta mye}$ mice following chronic *H. pylori* infection.

ODC Deletion Promotes Histone Modifications Leading to Euchromatin Formation and Transcription. To this point, our studies have implicated ODC in macrophages as a major regulator of gastric inflammation, cytokine, and chemokine production and M1 macrophage activation. Overall, our data indicate that mice with *Odc*-deficient macrophages exhibit a substantial increase in proinflammatory gene transcription. Previous studies have demonstrated that both ODC and the polyamines generated

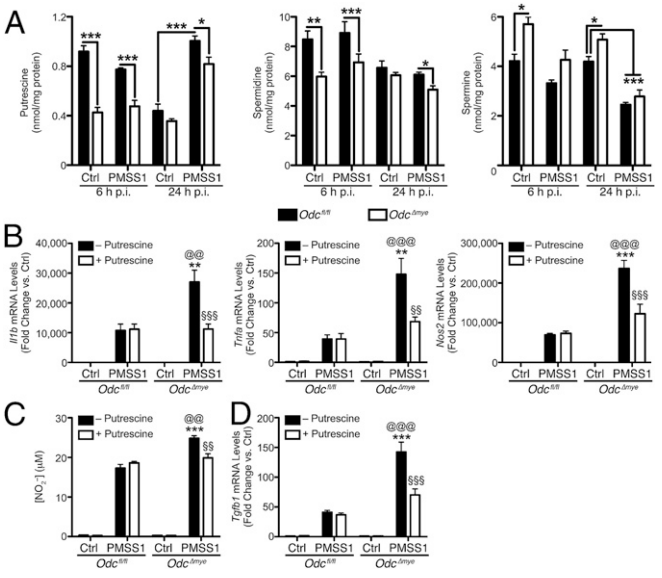

Fig. 4. The effects of *Odc* deletion in macrophages are due to putrescine depletion. (*A*) Measurement of polyamine levels in BMmacs 6 h and 24 h p.i. with *H. pylori* PMSS1 by mass spectrometry. ***$P < 0.001$ by one-way ANOVA with Newman–Keuls posttest. $n = 3$–4 mice per genotype. (*B*) mRNA levels of M1 cytokines *Il1b*, *Tnfa*, and *Nos2* were assessed by RT-PCR in BMmacs 24 h p.i. with *H. pylori* PMSS1 ± 25 μM putrescine added 60 min before infection. (*C*) Measurement of NO_2^- from BMmac supernatants 24 h p.i. with *H. pylori* PMSS1 ± 25 μM putrescine added 60 min before infection. (*D*) mRNA levels of the M2 cytokine, *Tgfb1*, were assessed by RT-PCR in BMmacs 24 h p.i. with *H. pylori* PMSS1 ± 25 μM putrescine added 60 min before infection. In *B*–*D*, **$P < 0.01$, ***$P < 0.001$ vs. $Odc^{fl/fl}$ + PMSS1; $^{@@}P < 0.01$, $^{@@@}P < 0.001$ vs. $Odc^{fl/fl}$ + PMSS1 + putrescine; $^{§§}P < 0.01$, $^{§§§}P < 0.001$ vs. $Odc^{\Delta mye}$ + PMSS1 by one-way ANOVA with Newman–Keuls posttest. $n = 4$ biological replicates. Data are displayed as mean ± SEM.

have the ability to influence histone modifications and, therefore, regulate gene transcription (50, 51). To gain an understanding of the role of ODC in altering macrophage gene transcription in response to bacterial infection, we assessed histone modifications at histone 3, lysine 4 (H3K4), known to be found at enhancer regions (52), as well as H3K9, which is a specific residue known to mark global alterations in chromatin structure and gene transcription levels (53). Specifically, H3K4 monomethylation (H3K4me1) is associated with primed, active enhancers and up-regulated transcriptional levels (52). H3K9 acetylation (H3K9ac) is associated with euchromatin formation and increased gene expression, whereas H3K9 di/trimethylation (H3K9me2/3) is associated with heterochromatin formation and decreased gene expression (53). Under conditions of *H. pylori* infection, $Odc^{\Delta mye}$ BMmacs demonstrated significantly increased H3K4me1 and H3K9ac levels and decreased H3K9me2/3 levels versus $Odc^{fl/fl}$ BMmacs (Fig. 5 *A* and *B*), indicative of enhanced gene transcription and correlating with the observed alterations in macrophage activation patterns in the present study. Importantly, a marked increase in H3K9 acetylation was noted in $CD68^+$ gastric macrophages from *H. pylori*-infected $Odc^{\Delta mye}$ mice versus *H. pylori*-infected $Odc^{fl/fl}$ mice (Fig. 5*C*). Similar alterations in H3K9 acetylation and methylation were observed in *C. rodentium*-infected BMmacs (*SI Appendix*, Fig. S15). Intriguingly, these changes in H3K4me1, H3K9ac, and H3K9me2/3 levels only significantly occurred upon *H. pylori* or *C. rodentium* infection, implying that the alterations in histone modifications are specific to the macrophage response to stimulation and not occurring during basal conditions.

As with the expression of markers of M1 macrophage and NLRP3-inflammasome activation, the addition of putrescine reversed the histone modifications in $Odc^{\Delta mye}$ BMmacs, such that they then resembled the H3K9ac and H3K9me2/3 levels in $Odc^{fl/fl}$ BMmacs during *H. pylori* infection (*SI Appendix*, Fig. S16). The addition of excess spermidine or spermine, the other two principal polyamines, did not change H3K9ac or H3K9me2/3 levels in either $Odc^{fl/fl}$ or $Odc^{\Delta mye}$ BMmacs (*SI Appendix*, Fig. S16), indicating that putrescine plays a more critical role in regulating histone modifications during *H. pylori* infection in macrophages.

To verify that the loss of ODC in macrophages was directly affecting transcription of the proinflammatory M1 markers through H3K9 alterations, namely enhanced acetylation and diminished methylation, we performed chromatin immunoprecipitation (ChIP), followed by RT-PCR in $Odc^{fl/fl}$ and $Odc^{\Delta mye}$ BMmacs. ChIP was performed with both anti-H3K9ac and anti-H3K9me3 antibodies to assess gene expression during both chromatin modifications. Immunoprecipitation with an anti-H3K9ac antibody resulted in significantly increased glyceraldehyde 3-phosphate dehydrogenase (*Gapdh*) expression in *H. pylori*-infected $Odc^{\Delta mye}$ BMmacs (Fig. 5*D*). *Gapdh* expression is a marker of transcriptionally active euchromatin (54). *Gapdh* was not substantially immunoprecipitated with an anti-H3K9me3 antibody (*SI Appendix*, Fig. S17*A*), consistent with this gene representing a marker of euchromatin rather than heterochromatin. Inversely, immunoprecipitation with an anti-H3K9me3 antibody demonstrated significantly decreased expression of inhibitor of apoptosis (*Iap*), a marker indicative of heterochromatin (55), in *H. pylori*-infected $Odc^{\Delta mye}$ BMmacs versus *H. pylori*-infected $Odc^{fl/fl}$ BMmacs (Fig. 5*D*). Moreover, *Iap* was not markedly immunoprecipitated with an anti-H3K9ac antibody (*SI Appendix*, Fig. S16*A*). *Myod1* is indicative of transcriptionally inactive euchromatin (54) and was unchanged between genotypes with immunoprecipitation with either antibody (*SI Appendix*, Fig. S17*B*). Taken together, these data demonstrate that the loss of ODC leads to an enhancement in transcriptionally active euchromatin levels during infection and a decrease in heterochromatin levels, which would result in enhanced gene transcription.

To test whether alterations in chromatin modifications were specifically modulating proinflammatory gene expression, we also assessed *Il1b*, *Il6*, *Tnfa*, and *Nos2* promoter levels by ChIP-PCR. *Il1b*, *Il6*, *Tnfa*, and *Nos2* promoter levels were significantly increased in $Odc^{\Delta mye}$ BMmacs versus $Odc^{fl/fl}$ BMmacs during H3K9ac immunoprecipitation (Fig. 5*E*) and were not significantly immunoprecipitated with an anti-H3K9me3 antibody (*SI Appendix*, Fig. S18). Taken together, these data verify that chromatin alterations during *Odc* deletion in macrophages drive enhanced proinflammatory gene expression, which then contributes to increased immune cell activation, exhibited as enhanced histologic gastritis that leads to diminished *H. pylori* bacterial burden.

ODC-Driven Histone Modifications Are Essential for Alterations in M1 Macrophage Activation. Finally, to determine whether histone modifications, specifically methylation and acetylation events, are the mechanism by which the loss of ODC alters M1 macrophage activation, we used pharmacological inhibitors of histone methylation and acetylation in $Odc^{fl/fl}$ and $Odc^{\Delta mye}$ BMmacs and assessed expression of M1 macrophage activation markers.

BIX 01924 is a selective inhibitor of euchromatic histone lysine methyltransferase 2 (EHMT2; also known as G9a histone methyltransferase), which is known to interact specifically with H3K9 (56). We hypothesized that inhibition of EHMT2 would remove the inhibitory methylation present in $Odc^{fl/fl}$ BMmacs, leading to increased expression of M1 macrophage activation markers. Indeed, BIX 01924 treatment resulted in significantly increased *Il1b*, *Tnfa*, and *Nos2* expression in $Odc^{fl/fl}$ BMmacs during *H. pylori* infection (Fig. 6*A*). As expected, treatment with BIX 01924 did not significantly alter M1 marker expression in $Odc^{\Delta mye}$ BMmacs (Fig. 6*A*). Moreover, BIX 01924 treatment did not alter M2 macrophage activation marker expression in either genotype (*SI Appendix*, Fig. S19*A*). These data further support the concept that the

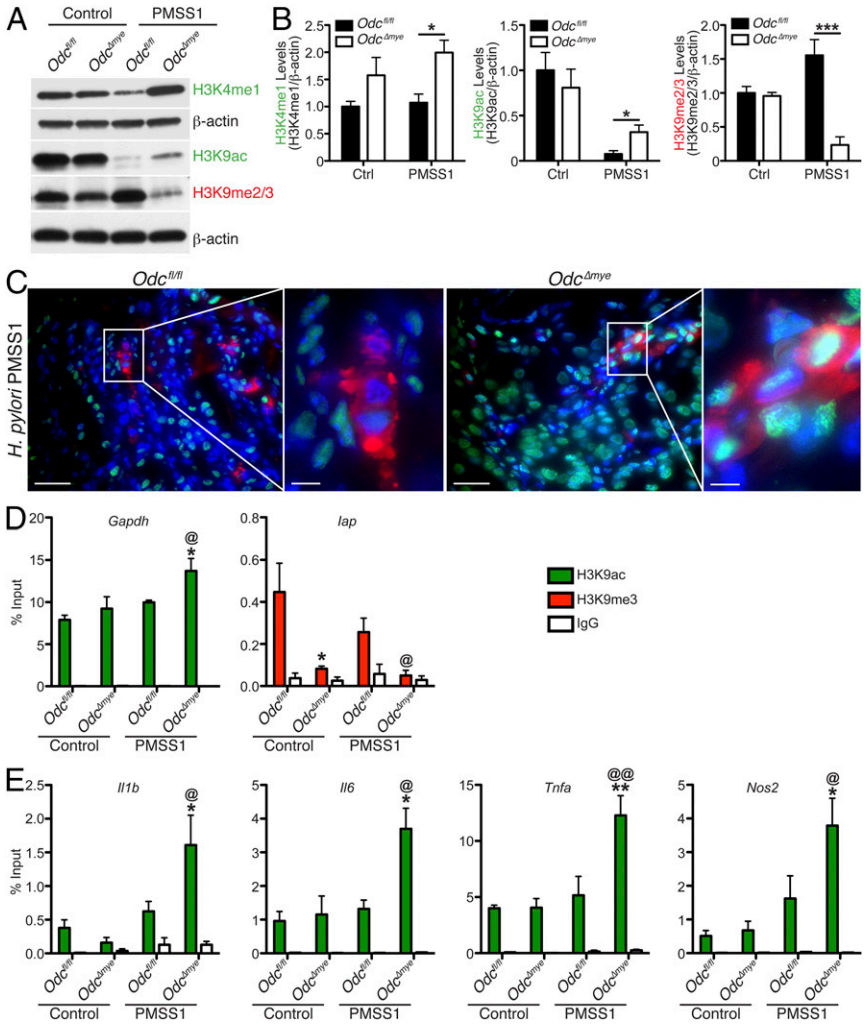

Fig. 5. *Odc* deletion in macrophages alters H3K4 and H3K9 modifications during *H. pylori* infection. (*A*) Representative Western blot of H3K4me1, H3K9ac, and H3K9me2/3 levels in BMmacs 24 h p.i. with *H. pylori* PMSS1. $n = 3$ biological replicates. (*B*) Densitometric analysis of H3K4me1, H3K9ac, and H3K9me2/3 levels in *A*. $*P < 0.05$, $***P < 0.001$ by one-way ANOVA with Newman–Keuls posttest. $n = 3$ biological replicates. (*C*) Representative immunofluorescence images of H3K9ac in *H. pylori*-infected gastric tissues 4 mo. p.i. Green, H3K9ac; red, CD68; and blue, DAPI. (Scale bars, 50 μm.) Boxed area indicates image shown at higher magnification. (Scale bar, 10 μm.) $n = 3$ biological replicates per genotype. Note that a cell is considered double positive if the cell surface is red and the nucleus is green. (*D*) Expression of *Gapdh* and *Iap* was assessed by RT-PCR in BMmacs from $Odc^{fl/fl}$ and $Odc^{\Delta mye}$ mice 24 h p.i. with *H. pylori* PMSS1 with subsequent ChIP with the denoted antibodies. $*P < 0.05$. $n = 3$ biological replicates. (*E*) Expression of *Il1b*, *Il6*, *Tnfa*, and *Nos2* promoter sequences was assessed by RT-PCR in BMmacs from $Odc^{fl/fl}$ and $Odc^{\Delta mye}$ mice 24 h p.i. with *H. pylori* PMSS1 with subsequent ChIP with the denoted antibodies. $*P < 0.05$. $n = 3$ biological replicates. In *D* and *E*, statistical significance was calculated by one-way ANOVA with Newman–Keuls posttest on square-root transformed data. Data are displayed as mean ± SEM.

loss of ODC in the $Odc^{\Delta mye}$ BMmacs allowed for potentiation of M1 marker expression by relieving the methylation of H3K9, therefore leading to increased immune response and gastric inflammation.

Anacardic acid is a selective inhibitor of lysine acetyltransferase 2A (KAT2A; also known as GCN5), which has been previously shown to interact with H3K9 (57). Inhibition of KAT2A significantly reduced M1 marker expression in $Odc^{\Delta mye}$ BMmacs, such that expression was similar to M1 marker expression in $Odc^{fl/fl}$ BMmacs during *H. pylori* infection (Fig. 6*B*). Anacardic acid treatment did not alter M1 marker gene expression in *H. pylori*-infected $Odc^{fl/fl}$ BMmacs (Fig. 6*B*). Additionally, anacardic acid did not alter the expression of M2 macrophage markers, again indicating that the role of ODC in regulating histone modifications is specific to the M1 response (*SI Appendix*, Fig. S19*B*).

Taken together, these studies demonstrate that loss of ODC in macrophages leads to an M1 response that is driven by ODC/putrescine-mediated histone modifications that alter chromatin structure and the capacity for active gene transcription. This increased M1 response is a key orchestrator of the increased gastric inflammatory response.

Discussion

ODC and polyamines have been well studied in epithelial cells within the context of cancer and in macrophages within the context of parasitic and fungal infections. The present study now reveals a mechanism by which ODC and its product, putrescine, regulate M1 macrophage activation via alterations of histone modifications to directly alter proinflammatory gene expression during bacterial infection. We demonstrate that loss of ODC in macrophages has profound effects on M1 macrophage activation and thus, on the pathogenesis of both *H. pylori* and *C. rodentium* in mice. We further demonstrate that deletion of ODC leads to alterations in *H. pylori* survival during gastric infection, implicating ODC in macrophages as a mediator of bacterial persistence within a host. This is a critical advancement of our understanding of the immune

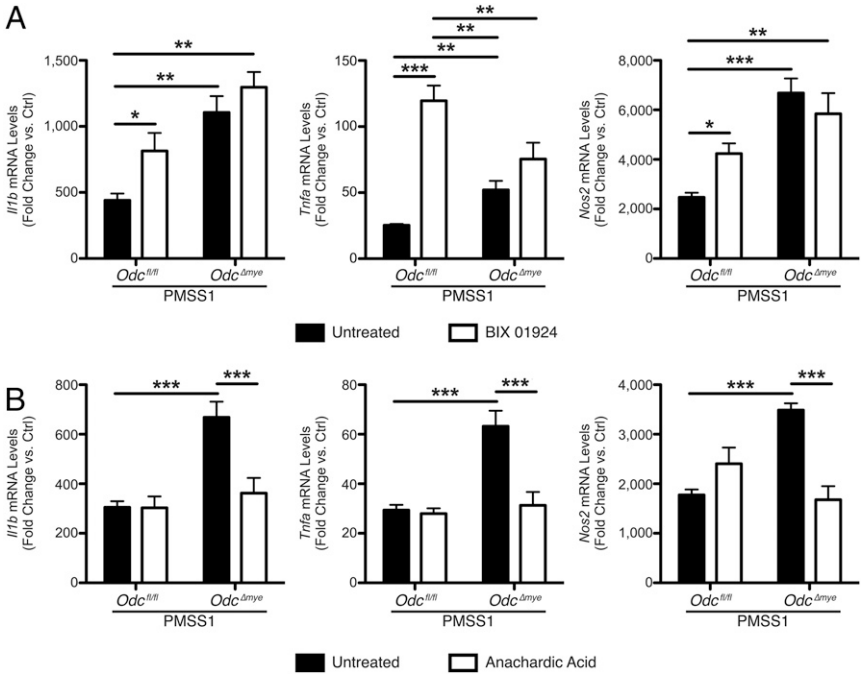

Fig. 6. Alterations in histone modifications and chromatin structure in ODC-deficient macrophages alters M1 macrophage activation during *H. pylori* infection. (*A*) mRNA levels of proinflammatory cytokines *Il1b*, *Tnfa*, and *Nos2* were assessed by RT-PCR in BMmacs 24 h p.i. with *H. pylori* PMSS1 ± 5 μM BIX 01924 added 60 min before infection. $*P < 0.05$, $**P < 0.01$, $***P < 0.001$ by one-way ANOVA with Kruskal–Wallis test, followed by Mann–Whitney *u* test. $n = 5$ mice per genotype. (*B*) mRNA levels of proinflammatory cytokines *Il1b*, *Tnfa*, and *Nos2* were assessed by RT-PCR in BMmacs 24 h p.i. with *H. pylori* PMSS1 ± 10 μM anacardic acid added 60 min before infection. $***P < 0.001$ by one-way ANOVA with Kruskal–Wallis test, followed by Mann–Whitney *u* test. $n = 5$ mice per genotype. Data are displayed as mean ± SEM.

privilege that is associated with this particular infection, as long-term persistence is the hallmark of *H. pylori* infection and is directly linked to damaging inflammation and increased cancer risk (31, 33, 34).

ODC is detectable in abundance in human gastric myeloid cells during *H. pylori* infection, indicating the potential importance of the enzyme in regulating the host response to the pathogen (25). Previous studies demonstrated that pharmacologic inhibition of ODC with DFMO diminished both inflammation and *H. pylori* colonization in mice (25, 38), although it should be noted that we have shown that DFMO can have direct inhibitory effects on *H. pylori* (38). Based on the robust induction of ODC in macrophages during *H. pylori* infection (24), we anticipated that myeloid-specific deletion of ODC might result in decreased inflammation and decreased colonization. However, we observed significantly increased inflammation, accompanied by a reduction in *H. pylori* colonization. We attribute this finding to dramatically enhanced M1 macrophage activation, up-regulated cytokine and chemokine expression, and significantly increased production of NO, which is a potent antimicrobial mediator. Clearly, ODC expression in macrophages actually impairs the host response. The ability of *H. pylori* to up-regulate ODC, via ERK and MYC signaling (6, 24), is advantageous for the creation of a less inflammatory environment in which the pathogen can establish a persistent infection. However, even in the tolerant environment, persistent infection is still accompanied by chronic inflammation, leading to increased risk for gastric cancer (32–34). Thus, inhibition of ODC may prove to be a potential target to enhance the clearance of long-term infection.

C. rodentium-infected $Odc^{\Delta mye}$ mice also had substantially increased disease severity, again attributable to increased M1 macrophage activation. Several previous studies have demonstrated that the severity of colitis is positively correlated with *C. rodentium* colonization (26, 45, 58, 59). The fact that colonization was not different in our model, despite increased colitis, potentially indicates that colonization was actually impaired, as we would have expected increased colonization accompanying increased colitis. The concordance in macrophage activation patterns and histologic inflammation between the *H. pylori* and *C. rodentium* models in our study, combined with the studies with classical M1 and M2 stimuli, indicate that the role of ODC in macrophages is broadly applicable across various models of mucosal inflammation and is an important mediator of general macrophage activation and biology in mice and humans.

ODC serves as such a potent mediator of macrophage function via its role in the alteration of chromatin structure and gene transcription. ODC and polyamines are known to modulate chromatin modifications, DNA stability, and gene expression (3–5). However, we have now demonstrated that ODC and polyamines have the ability to directly regulate the expression of proinflammatory genes within the context of bacterial infections. This is a critical expansion of our understanding of macrophage activation and function. Putrescine is the product of the enzymatic conversion of L-ornithine by ODC. In our study, putrescine, but not spermidine or spermine, was capable of reversing the activation patterns observed in $Odc^{\Delta mye}$ BMmacs infected with either *H. pylori* or *C. rodentium*. These studies indicate that putrescine is a potent regulatory molecule in macrophage activation. Further studies are required to determine the mechanism by which putrescine modulates histone modifications.

In summary, our work outlines a role for ODC in regulating macrophage activation during bacterial infections. ODC is a well-known mediator of cancer risk across various types of cancer, including gastric and colorectal cancers (7–11). Importantly, chronic inflammation contributes to the process of carcinogenesis and we now implicate ODC as having a role in the establishment of chronic inflammation by tempering the M1 macrophage response to bacterial pathogens. A finding in the current study is that these

phenotypes are due to the alteration of chromatin structures by modifications of putrescine levels within macrophages. These studies provide further impetus for studies related to the role of ODC in macrophages as a potential pathway to better understanding the etiology, prevention, and treatment of inflammatory diseases and associated cancer risk.

Methods

Materials/Reagents. All reagents used for cell culture were from Invitrogen. Reagents for RNA extraction are from Qiagen. Reagents for cDNA synthesis and RT-PCR were purchased from Bio-Rad. The following reagents were obtained from PeproTech: murine recombinant M-CSF, murine recombinant IFN-γ, and murine recombinant IL-4. The following reagents were obtained from Sigma-Aldrich: LPS from *E. coli* O111:E4, anacardic acid (2-hydroxy-6-pentadecylbenzoic acid, 6-pentadecylsalicylic acid), putrescine, spermine, spermidine, putrescine-d_4 (1,4-diaminobutane-2,2,3,3-d_4 dihydrochloride), spermidine-d_8 [spermidine-(butane-d_8) trihydrochloride], and spermine-d_8 [spermine-(butane-d_8) tetrahydrochloride]. Dansyl chloride was obtained from Acros Organics. BIX 01924 {2-(hexahydro-4-methyl-1*H*-1,4-diazepin-1-yl)-6,7-dimethoxy-*N*-[1-(phenylmethyl)-4-piperidinyl]-4-quinazolinamine trihydrochloride} was obtained from Fisher Scientific.

Antibodies. See *SI Appendix*, Table S2 for information regarding antibodies used for this study.

Bacteria, Cells, Culture Conditions, and Infections. *H. pylori* PMSS1 and SS1 were cultured as previously described (25, 42). PMSS1 was used for acute in vivo and ex vivo infections because it is the original clinical isolate and retains its ability to translocate the oncoprotein, CagA. SS1 was used for chronic infections in vivo because of its ability to induce robust gastritis in mice. *C. rodentium* was cultured as previously described (35).

Bone-marrow–derived macrophages were isolated and differentiated as previously described (14). Upon completion of differentiation, cells were placed in complete DMEM, supplemented with 10% (50 mL FBS/500 mL DMEM) FBS, 2 mM L-glutamine, 25 mM Hepes, and 10 mM sodium pyruvate for studies with *H. pylori* or *C. rodentium* infection. THP1 cells were maintained in complete DMEM, supplemented with 10% (50 mL FBS/500 mL DMEM) FBS, 2 mM L-glutamine, 25 mM Hepes, and 10 mM sodium pyruvate. No antibiotics were present in media during bacterial infections.

All pharmacological inhibitors (except DFMO) or polyamines were added 1 h before infection. Cells were infected at a multiplicity of infection (MOI) of 100 for *H. pylori* studies and at a MOI of 10 for *C. rodentium* studies. All infection studies were performed with live bacteria.

Animal Studies. $Odc^{fl/fl}$ mice were generated and provided by J.L.C. $Odc^{\Delta mye}$ mice were generated by crossing $Odc^{fl/fl}$ mice with $LysM^{cre/cre}$ mice from our stock of breeding colonies. Animals were used under protocol M/10/155, approved by the Institutional Animal Care and Use Committee at Vanderbilt University.

Male mice between the ages of 6 and 12 wk were used for all studies within this paper. Mice were not removed from the cages into which they were weaned. Male mice were selected because previous studies have demonstrated that female mice are protected from gastric damage during *H. pylori* infection (60). Sample sizes were based on previous studies (14, 25, 42, 61). No other selection criteria were used in these studies. Mice were infected orogastrically with 5×10^8 cfus of *H. pylori* SS1 every other day for three total inoculations for the 4-mo infections or with 5×10^8 cfus of *H. pylori* PMSS1 once for 48-h infections. Mice were infected orogastrically with 5×10^8 cfus of *C. rodentium* once for 14-d infections. All bacteria were in log phase for infections. Animals were killed at indicated time points. Colonization, histologic gastritis, and histologic colitis were assessed as previously described (14, 23), as appropriate to the infection model. All histologic assessments were made in a blinded manner by a gastrointestinal pathologist (M.B.P.).

On rare occasions, $Odc^{\Delta mye}$ and $LysM^{cre/cre}$ mice would develop a substantially enlarged spleen that was not attributable to *H. pylori* or *C. rodentium* infection, as control mice would also manifest this condition. If marked splenomegaly was observed at time of killing, that mouse was excluded from further analysis.

Real-Time PCR. RNA was isolated from cells and tissues, cDNA was prepared, and PCR was performed as previously described (14, 23). See *SI Appendix*, Table S3 for primers used in this study.

Western Blot Analysis. Western blot analysis was performed as previously described (14). See *SI Appendix*, Table S2 for all antibodies used in this study with accompanying information regarding dilutions used.

Luminex Multiplex Array. Luminex multiplex array was performed as previously described (14).

ELISAs. The following R&D DuoSet ELISA kits were used for cytokine measurements: IL-1β (DY401), TNF-α (DY410), IL-6 (DY406), IL-12p70 (DY419), IL-10 (DY417), and TGF-β1 (DY1679). All ELISAs were performed according to kit instructions.

Measurement of Nitric Oxide. The concentration of the oxidized metabolite of NO, nitrite (NO_2^-) was assessed by the Griess reaction as previously described (14).

DFMO Studies in THP1 Cells. THP1 cells were treated with 5 mM DFMO in T-75 flasks for 3 or 5 d. Cells were then counted, plated, and treated with 10 ng/mL PMA for 18 h to differentiate the cells into macrophages. A total of 5 mM DFMO was maintained in the media during PMA treatment. Following differentiation, cells were place in antibiotic-, PMA-, and DFMO-free media and infected with *H. pylori* PMSS1 (MOI, 100) for 6 h. All RNA and protein assays were performed as described above.

Immunofluorescence Staining for ODC, CD68, and H3K9ac in Murine Tissues. Immunofluorescence staining for ODC, CD68, and H3K9ac in murine tissues was performed using a staining protocol that was previously described (14), with the following alterations. As the source for each of the three antibodies is rabbit, tissues were blocked with 5% goat serum and rabbit Fab fragment for 30 min at room temperature following incubation in primary and secondary antibodies for either ODC or H3K9ac before incubation with anti-CD68. A secondary anti-rabbit antibody with an Alexa 488 tag was used. Slides were imaged using a SPOT RT slider camera system (Diagnostic Instruments) on a Nikon E800 microscope (Nikon). Images were all modestly adjusted in ImageJ with the brightness and contrast tool.

Immunoperoxidase Staining for ODC. Staining for ODC in human gastric biopsies was performed as previously described (25).

Immunofluorescence Staining for ODC and CD68 Human Tissues. Immunofluorescence staining for ODC and CD68 in human tissues was performed using a staining protocol that was previously described (14). Quantification of $CD68^+$ ODC^+ and $CD68^+ODC^-$ cells was performed by four blinded observers and the scoring was averaged.

Human Tissues. Deidentified human gastric samples from Colombia were obtained and used as previously described (14). All patients participating in studies in Colombia were enrolled with informed consent, and the deidentified coded tissues were provided under nonhuman exemptions approved by the Vanderbilt University Institutional Review Board.

Purification of Gastric Epithelial Cells and Gastric Macrophages. Purification of gastric epithelial cells and gastric macrophages was performed as previously described (14).

Measurement of Polyamines. All studies related to polyamine measurements were conducted in serum-free media. Putrescine, spermidine, and spermine were quantified by LC-MS using a Thermo TSQ Vantage Triple Quadrupole instrument operated in positive ion mode. Cell pellets were extracted using acetonitrile/20 mM NH_4OAc pH 8 (70:30). Extracts were derivatized by reaction with 20 mM dansyl chloride in 100 mM $NaHCO_3$ pH 10 for 20 min. Polyamines were quantified using deuterated internal standards d_4-putrescine, d_8-spermidine, and d_8-spermine.

ChIP-PCR. ChIP was performed using the EpiTect Chip ChIP-Grade Antibody Kit (H3K9ac) (Qiagen, cat. no. GAM-1209) and the EpiTect Chip ChIP-Grade Antibody Kit (H3K9me3) (Qiagen, cat. no. GAM-6204). All reagents were provided in the EpiTect Chip One-Day Kit (Qiagen, cat. no. 334471). All kit instructions were followed as stated, including PCR master mix set-up and recommended PCR protocol. Primers for *Gapdh* and *Myod1* were provided with the ChIP antibody kits listed above. Primers for *Il1b*, *Il6*, *Tnfa*, and *Nos2* promoter sites are listed in *SI Appendix*, Table S3.

Statistical Analysis. All of the data shown represent the mean ± SEM. At least three biological replicates were performed for all studies using cell culture. Where data were normally distributed, two-tailed Student's *t* test was used to determine significance in experiments with only two groups, and one-way ANOVA with the Newman–Keuls test was used to determine significant differences between multiple test groups. In cases where data were not normally distributed, a one-way ANOVA with Kruskal–Wallis test, followed by a Mann–Whitney *u* test, was performed, unless otherwise noted. All

statistics were performed in GraphPad Prism 5.0 (GraphPad Software). A P value of <0.05 was considered to be significant.

ACKNOWLEDGMENTS. We thank Margaret M. Allaman (Vanderbilt University) for her assistance with the Luminex multiplex array and David Feith (University of Virginia) and Lisa Shantz (Pennsylvania State College of Medicine) for providing the ODC antibody. This work was funded by NIH Grants R01DK053620, R01AT004821, R01CA190612, P01CA116087, and P01CA028842 (to K.T.W.); R01AT006896 (to C.S.); Department of Veterans Affairs Merit Review Grant I01BX001453 (to K.T.W.); the Vanderbilt Digestive Disease Research Center (NIH Grant P30DK058404); the Thomas F. Frist Sr. Endowment (K.T.W.); and the Vanderbilt Center for Mucosal Inflammation and Cancer (A.P.G. and K. T.W.). Mass spectrometry was supported by the Vanderbilt Ingram Cancer Center (NIH Grant P30CA068485). D.M.H. was supported by NIH Grants T32GM008554 and F31DK10715. P.B.L. was supported by 16POST27250138 from the American Heart Association.

1. Pegg AE (2009) Mammalian polyamine metabolism and function. *IUBMB Life* 61(9): 880–894.
2. Pegg AE (2006) Regulation of ornithine decarboxylase. *J Biol Chem* 281(21): 14529–14532.
3. Hobbs CA, Gilmour SK (2000) High levels of intracellular polyamines promote histone acetyltransferase activity resulting in chromatin hyperacetylation. *J Cell Biochem* 77(3):345–360.
4. Brooks WH (2013) Increased polyamines alter chromatin and stabilize autoantigens in autoimmune diseases. *Front Immunol* 4:91.
5. Huang Y, Marton LJ, Woster PM, Casero RA (2009) Polyamine analogues targeting epigenetic gene regulation. *Essays Biochem* 46:95–110.
6. Asim M, et al. (2010) *Helicobacter pylori* induces ERK-dependent formation of a phospho-c-Fos c-Jun activator protein-1 complex that causes apoptosis in macrophages. *J Biol Chem* 285(26):20343–20357.
7. Wallace HM, Fraser AV (2004) Inhibitors of polyamine metabolism: Review article. *Amino Acids* 26(4):353–365.
8. Soda K (2011) The mechanisms by which polyamines accelerate tumor spread. *J Exp Clin Cancer Res* 30:95.
9. Linsalata M, Orlando A, Russo F (2014) Pharmacological and dietary agents for colorectal cancer chemoprevention: Effects on polyamine metabolism (review). *Int J Oncol* 45(5):1802–1812.
10. Gerner EW, Meyskens FL, Jr (2004) Polyamines and cancer: Old molecules, new understanding. *Nat Rev Cancer* 4(10):781–792.
11. Casero RA, Jr, Marton LJ (2007) Targeting polyamine metabolism and function in cancer and other hyperproliferative diseases. *Nat Rev Drug Discov* 6(5):373–390.
12. Mosser DM, Edwards JP (2008) Exploring the full spectrum of macrophage activation. *Nat Rev Immunol* 8(12):958–969.
13. Mosser DM (2003) The many faces of macrophage activation. *J Leukoc Biol* 73(2): 209–212.
14. Hardbower DM, et al. (2016) EGFR regulates macrophage activation and function in bacterial infection. *J Clin Invest* 126(9):3296–3312.
15. Fleming BD, Mosser DM (2011) Regulatory macrophages: Setting the threshold for therapy. *Eur J Immunol* 41(9):2498–2502.
16. Martinez FO, Gordon S (2014) The M1 and M2 paradigm of macrophage activation: Time for reassessment. *F1000Prime Rep* 6:13.
17. Ostuni R, Kratochvill F, Murray PJ, Natoli G (2015) Macrophages and cancer: From mechanisms to therapeutic implications. *Trends Immunol* 36(4):229–239.
18. Anderson CF, Mosser DM (2002) A novel phenotype for an activated macrophage: The type 2 activated macrophage. *J Leukoc Biol* 72(1):101–106.
19. Seabra SH, DaMatta RA, de Mello FG, de Souza W (2004) Endogenous polyamine levels in macrophages is sufficient to support growth of Toxoplasma gondii. *J Parasitol* 90(3):455–460.
20. Liao CP, et al. (2009) Pneumocystis mediates overexpression of antizyme inhibitor resulting in increased polyamine levels and apoptosis in alveolar macrophages. *J Biol Chem* 284(12):8174–8184.
21. Heby O, Persson L, Rentala M (2007) Targeting the polyamine biosynthetic enzymes: A promising approach to therapy of African sleeping sickness, Chagas' disease, and leishmaniasis. *Amino Acids* 33(2):359–366.
22. Van den Bossche J, et al. (2012) Pivotal Advance: Arginase-1-independent polyamine production stimulates the expression of IL-4-induced alternatively activated macrophage markers while inhibiting LPS-induced expression of inflammatory genes. *J Leukoc Biol* 91(5):685–699.
23. Hardbower DM, et al. (2016) Arginase 2 deletion leads to enhanced M1 macrophage activation and upregulated polyamine metabolism in response to *Helicobacter pylori* infection. *Amino Acids* 48(10):2375–2388.
24. Cheng Y, et al. (2005) *Helicobacter pylori*-induced macrophage apoptosis requires activation of ornithine decarboxylase by c-Myc. *J Biol Chem* 280(23):22492–22496.
25. Chaturvedi R, et al. (2010) Polyamines impair immunity to *Helicobacter pylori* by inhibiting L-arginine uptake required for nitric oxide production. *Gastroenterology* 139(5):1686–1698, 1698.e1–1698.e6.
26. Gobert AP, et al. (2004) Protective role of arginase in a mouse model of colitis. *J Immunol* 173(3):2109–2117.
27. Cover TL, Blaser MJ (2009) *Helicobacter pylori* in health and disease. *Gastroenterology* 136(6):1863–1873.
28. Nomura A, et al. (1991) *Helicobacter pylori* infection and gastric carcinoma among Japanese Americans in Hawaii. *N Engl J Med* 325(16):1132–1136.
29. Blaser MJ, et al. (1995) Infection with *Helicobacter pylori* strains possessing cagA is associated with an increased risk of developing adenocarcinoma of the stomach. *Cancer Res* 55(10):2111–2115.
30. Mera R, et al. (2005) Long term follow up of patients treated for *Helicobacter pylori* infection. *Gut* 54(11):1536–1540.
31. Hardbower DM, de Sablet T, Chaturvedi R, Wilson KT (2013) Chronic inflammation and oxidative stress: The smoking gun for *Helicobacter pylori*-induced gastric cancer? *Gut Microbes* 4(6):475–481.
32. Robinson K, Argent RH, Atherton JC (2007) The inflammatory and immune response to *Helicobacter pylori* infection. *Best Pract Res Clin Gastroenterol* 21(2):237–259.
33. Peek RM, Jr, Fiske C, Wilson KT (2010) Role of innate immunity in *Helicobacter pylori*-induced gastric malignancy. *Physiol Rev* 90(3):831–858.
34. Israel DA, Peek RM, Jr (2006) The role of persistence in *Helicobacter pylori* pathogenesis. *Curr Opin Gastroenterol* 22(1):3–7.
35. Singh K, et al. (2011) The apolipoprotein E-mimetic peptide COG112 inhibits NF-kappaB signaling, proinflammatory cytokine expression, and disease activity in murine models of colitis. *J Biol Chem* 286(5):3839–3850.
36. Kelly M, et al. (2006) Essential role of the type III secretion system effector NleB in colonization of mice by Citrobacter rodentium. *Infect Immun* 74(4):2328–2337.
37. Kaparakis M, et al. (2008) Macrophages are mediators of gastritis in acute *Helicobacter pylori* infection in C57BL/6 mice. *Infect Immun* 76(5):2235–2239.
38. Barry DP, et al. (2011) Difluoromethylornithine is a novel inhibitor of *Helicobacter pylori* growth, CagA translocation, and interleukin-8 induction. *PLoS One* 6(2):e17510.
39. Chaturvedi R, et al. (2015) Increased *Helicobacter pylori*-associated gastric cancer risk in the Andean region of Colombia is mediated by spermine oxidase. *Oncogene* 34(26):3429–3440.
40. de Sablet T, et al. (2011) Phylogeographic origin of *Helicobacter pylori* is a determinant of gastric cancer risk. *Gut* 60(9):1189–1195.
41. Algood HM, Gallo-Romero J, Wilson KT, Peek RM, Jr, Cover TL (2007) Host response to *Helicobacter pylori* infection before initiation of the adaptive immune response. *FEMS Immunol Med Microbiol* 51(3):577–586.
42. Lewis ND, et al. (2011) Immune evasion by *Helicobacter pylori* is mediated by induction of macrophage arginase II. *J Immunol* 186(6):3632–3641.
43. Noto JM, et al. (2013) Iron deficiency accelerates *Helicobacter pylori*-induced carcinogenesis in rodents and humans. *J Clin Invest* 123(1):479–492.
44. Van Kaer L, et al. (2014) CD8$\alpha\alpha^+$ innate-type lymphocytes in the intestinal epithelium mediate mucosal immunity. *Immunity* 41(3):451–464.
45. Williams CS, et al. (2013) MTG16 contributes to colonic epithelial integrity in experimental colitis. *Gut* 62(10):1446–1455.
46. Korn T, Bettelli E, Oukka M, Kuchroo VK (2009) IL-17 and Th17 Cells. *Annu Rev Immunol* 27:485–517.
47. DeLyria ES, Redline RW, Blanchard TG (2009) Vaccination of mice against H pylori induces a strong Th-17 response and immunity that is neutrophil dependent. *Gastroenterology* 136(1):247–256.
48. Lewis ND, et al. (2010) Arginase II restricts host defense to *Helicobacter pylori* by attenuating inducible nitric oxide synthase translation in macrophages. *J Immunol* 184(5):2572–2582.
49. Tschopp J, Schroder K (2010) NLRP3 inflammasome activation: The convergence of multiple signalling pathways on ROS production? *Nat Rev Immunol* 10(3):210–215.
50. Venkatesh S, Workman JL (2015) Histone exchange, chromatin structure and the regulation of transcription. *Nat Rev Mol Cell Biol* 16(3):178–189.
51. Voss TC, Hager GL (2014) Dynamic regulation of transcriptional states by chromatin and transcription factors. *Nat Rev Genet* 15(2):69–81.
52. Shlyueva D, Stampfel G, Stark A (2014) Transcriptional enhancers: From properties to genome-wide predictions. *Nat Rev Genet* 15(4):272–286.
53. Georgopoulos K (2002) Haematopoietic cell-fate decisions, chromatin regulation and ikaros. *Nat Rev Immunol* 2(3):162–174.
54. Mal A, Harter ML (2003) MyoD is functionally linked to the silencing of a muscle-specific regulatory gene prior to skeletal myogenesis. *Proc Natl Acad Sci USA* 100(4): 1735–1739.
55. Rangasamy D (2013) Distinctive patterns of epigenetic marks are associated with promoter regions of mouse LINE-1 and LTR retrotransposons. *Mob DNA* 4(1):27.
56. Tao H, et al. (2014) Histone methyltransferase G9a and H3K9 dimethylation inhibit the self-renewal of glioma cancer stem cells. *Mol Cell Biochem* 394(1–2):23–30.
57. Srivastava S, et al. (2014) Histone H3K9 acetylation level modulates gene expression and may affect parasite growth in human malaria parasite Plasmodium falciparum. *FEBS J* 281(23):5265–5278.
58. Bailey MT, et al. (2010) Stressor exposure disrupts commensal microbial populations in the intestines and leads to increased colonization by Citrobacter rodentium. *Infect Immun* 78(4):1509–1519.
59. Basu R, et al. (2012) Th22 cells are an important source of IL-22 for host protection against enteropathogenic bacteria. *Immunity* 37(6):1061–1075.
60. Sheh A, et al. (2011) 17β-estradiol and tamoxifen prevent gastric cancer by modulating leukocyte recruitment and oncogenic pathways in Helicobacter pylori-infected INS-GAS male mice. *Cancer Prev Res (Phila)* 4(9):1426–1435.
61. Gobert AP, et al. (2014) Heme oxygenase-1 dysregulates macrophage polarization and the immune response to *Helicobacter pylori*. *J Immunol* 193(6):3013–3022.